*Journal of Inclusion Phenomena and Molecular Recognition in Chemistry* **8**: 89–101, 1990.



# Formation and Decomposition of Gas Hydrates of Natural Gas Components*

P. ENGLEZOS, N. KALOGERAKIS, and P. R. BISHNOI**
*Department of Chemical and Petroleum Engineering, University of Calgary, Calgary, Alberta, Canada T2N 1N4*

(Received: 24 March 1988; in final form: 1 June 1988)

**Abstract.** Based on our theoretical and experimental work carried out during the last decade, our understanding of the thermodynamics and the kinetics of formation and decomposition of gas hydrates is presented. Hydrate formation is modelled as a crystallization process where two distinct processes (nucleation and growth) are involved. Prior to the nucleation the concentration of the gas in the liquid water exceeds that corresponding to the vapor–liquid equilibrium. This supersaturation is attributed to the extensive structural orientation in the liquid water and is necessary for the phase change to occur. The growth of the hydrate nuclei or the decomposition of a hydrate particle are modelled as two-step procedures. Only one adjustable parameter for each hydrate forming gas is required for the intrinsic rate of formation or decomposition. In addition the inhibiting effects of electrolytes or methanol on hydrate formation are discussed and experimental data on methane gas hydrate formation in the presence of aqueous solutions of 3% NaCl and 3% NaCl + 3% KCl, are presented along with the predicted values. Finally, the relevence of the ideas to the technological implications of gas hydrates as well as areas where future research is needed are discussed.

**Key words.** Crystallization, kinetics, electrolytes, gas hydrates, clathrate hydrates.

## 1. Introduction

The natural gas components (such as) methane, ethane, propane etc. form stable crystalline solid compounds with water commonly known as gas hydrates. They are formed in two cubic structures (I and II) and belong to a group of inclusion compounds called clathrates. The inclusion compounds have been thoroughly reviewed recently [1]. Natural gas hydrates are two- or multi-component non-stoichiometric compounds, where one component is always water. They are formed because water molecules, through hydrogen bonding, form a cage-like structure containing relatively large cavities which can be occupied by certain gas molecules whose molecular diameter is less than the diameter of the cavity. By the inclusion of the gaseous component, the structure which alone is thermodynamically unstable, becomes stabilized. The number and size of the cavities differ for the two structures; however, in both cases, the water molecules are tetrahedrally coordinated. The interactions between the host water molecules and the guest gaseous hydrate formers are usually weak and of the van der Waals type. Detailed information on the structural and physical properties of gas hydrates can be found in the literature [2, 3, 4]. Davidson and co-workers [5] have carried out interesting

* Dedicated to Dr D. W. Davidson in honor of his great contributions to the sciences of inclusion phenomena.

** Author for correspondence.

nuclear magnetic resonance investigations of many different hydrates. In addition, they point out [6] that methanol, which is a major hydrate formation inhibitor, does not enter the hydrate lattice.

Natural gas hydrates have significant technological importance. Major problems arise in natural gas transportation lines and hydrocarbon processing facilities which could be blocked or damaged by the formation of solid hydrates. On the other hand, gas hydrate formation offers possibilities in the development of water desalination and gas storage facilities. Finally, natural gas hydrates present a huge future hydrocarbon resource which may be commercially exploited given the right economic environment. In order to successfully exploit the technological implications of the gas hydrates, in addition to structural and physical property investigations, there is a strong need to understand and model the thermodynamics and the kinetics of gas hydrate formation and decomposition. In this paper, our understanding of the thermodynamics and the kinetics, based on our theoretical and experimental work carried out during the last decade, is presented. The relevance of the ideas to the technological problems is also discussed.

## 2. Thermodynamics of Gas Hydrates

One of the most important aspects of the gas hydrates thermodynamics is the calculation of the incipient hydrate formation conditions. The van der Waals–Platteeuw model [7], which describes the chemical potential of water in the solid hydrate state, is commonly used for such calculations. The model takes into account only host–guest interactions and has been successfully used to formulate computer implementable methodologies [8, 9, 10] to calculate the equilibrium conditions for systems of gas hydrates, natural gas components and water.

Gas hydrate formation in nature occurs in the presence of ground- or seawater. Electrolytes are not known to enter the hydrate lattice. Their presence, however, generally depresses the hydrate formation due to the alteration of the activity of water. Recently, a method has been proposed by Englezos and Bishnoi [11] to calculate the depression effects of single or mixed electrolytes. The method uses the van der Waals–Platteeuw model for the hydrate, Trebble–Bishnoi [12] equation of state for the gas phase, Pitzer's [13] or Meissner's [14] model for single electrolytes and Patwardhan and Kumar's model [15] for mixed electrolytes. The method is shown [11] to satisfactorily predict all experimental data available in the open literature on light hydrocarbon gases. In Figure 1 the predictions made by the method for the methane hydrate are shown together with recently obtained experimental data in our laboratory [16]. The concentrations shown in the figure are in weight per cent of the electrolytes. The method, however, is not applicable to gases which have significant solubilities in aqueous electrolyte solutions. Hence, further research is needed to develop new prediction methods for such systems.

Alcohols like methanol are also known to depress hydrate formation. Englezos *et al.* [17] have recently developed a method to calculate the depression effects of methanol using the Trebble–Bishnoi equation of state and the van der Waals–Platteeuw model. However, no satisfactory methods are available to calculate the hydrate formation conditions in systems containing methanol and aqueous electrolyte solutions.

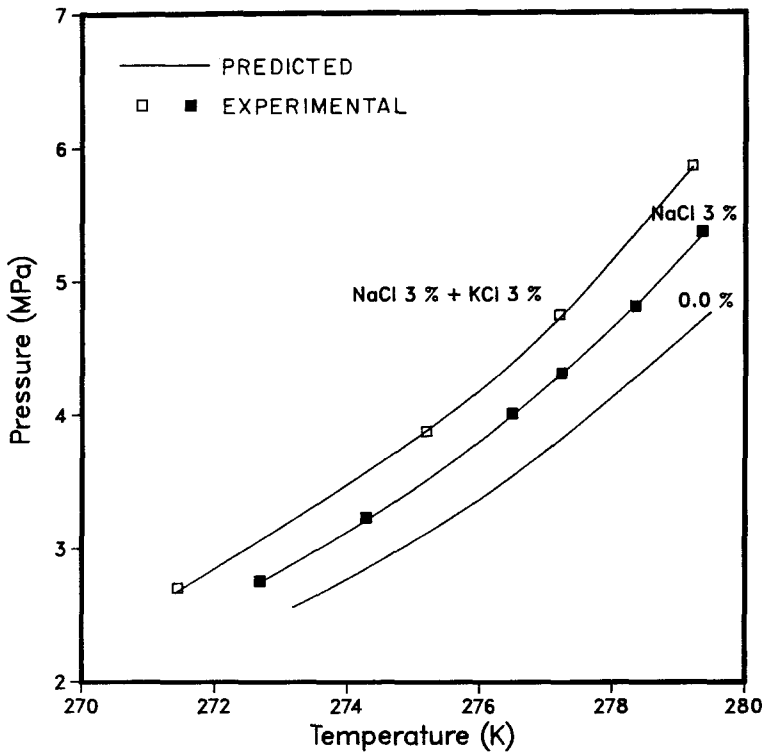


Fig. 1. Experimental and predicted pressures for methane gas hydrate formation from aqueous electrolyte solutions.

## 3. Solubility of Gases in Water, Supersaturation and Nucleation

Water molecules, linked through hydrogen bonding, tend to form a certain quasi-crystalline structure in the liquid state. The structure is lattice-like with cavities of molecular sizes. The lattice is thermodynamically unstable by itself at temperatures above the freezing point of water. The tendency, however, to form the structure is enhanced at temperatures near the freezing point, particularly in the presence of certain gases whose molecular diameter is smaller than the diameter of the cavity. At temperatures which are not too far above the freezing point of water, the structures can even become stable in the presence of such gases at sufficiently high pressures.

The tendency of the water molecules to form quasi-crystalline structures in the liquid state has some interesting ramifications. For example, the methane gas can be dissolved in the liquid water to obtain a supersaturated solution at a pressure higher than the hydrate formation pressure for a given temperature. The concentration of methane in the supersaturated solution can be even higher than the metastable vapor–liquid equilibrium concentration calculated by Henry's law or an equation of state at the system pressure and temperature. This supersaturation phenomenon has been experimentally observed in our laboratory. During the hydrate formation

experiments [18, 19, 20, 21] a gas is brought into contact with liquid water under isobaric and isothermal conditions and the amount of gas consumed is measured versus time. In Figure 2 the results from one such experiment are shown. Up to the point B gas simply dissolves in the liquid water phase. At point B the solution suddenly becomes translucent. This is observed visually and this point is marked as the nucleation or turbidity point. After that, as seen from the figure, the gas consumption continues due to hydrate formation. Also shown in the figure are the number of moles of methane corresponding to the three phase equilibrium conditions, $n_{eq}$, and the number of moles corresponding to the vapor–liquid equilibrium, $n^*$, which are calculated by the Trebble–Bishnoi equation of state. The concentration of the gas at the turbidity point, i.e., at supersaturation, is higher possibly because the gas molecules are enclosed in the cavities formed by the clusters of water molecules and as a result the bulk liquid phase is depleted in the gas molecules providing space for more gas molecules to be dissolved. The clusters of water molecules with the additional gas are growing and they reach a critical size when they become stable gas hydrate nuclei. The nuclei subsequently grow by enclathration of more gas molecules at the crystal–water interface. Due to energy considerations, it is most likely for a gas molecule to be enclathrated on an existing hydrate particle rather than be consumed for the formation of a new nucleus. The

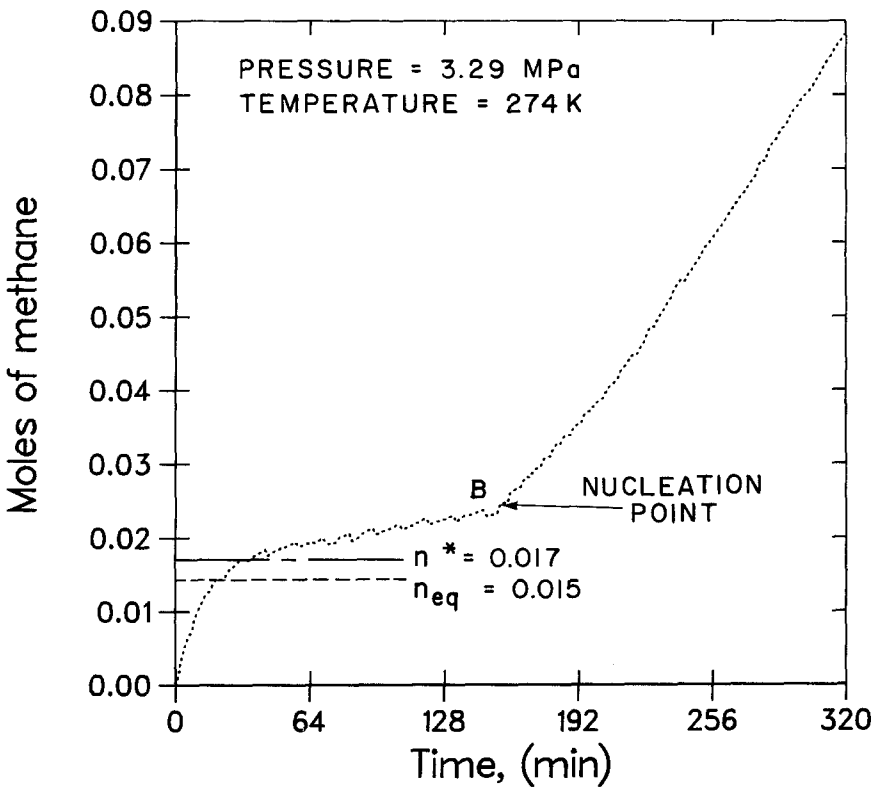


Fig. 2. Experimental gas consumption curve for methane hydrate formation in a semi-batch reactor containing 300 $cm^3$ of distilled water.

lattice-like structure of water can also be seen as a porous material acting as an adsorbent. Crystallization occurs by the adsorption of gas molecules with simultaneous stabilization of the cavity [22]. Crystallization is a process characterized by two distinct phenomena, namely nucleation and growth. Local supersaturation of the liquid solution is necessary prior to the formation of the nuclei. When the liquid water is free from foreign particles, nucleation is primarily homogeneous. Under these conditions the critical size of the hydrate nucleus can be calculated from thermodynamic considerations [20, 21].

The limits of intrinsic thermodynamic stability for a binary solution can be easily calculated by Gibbs free energy analysis. These limits have been calculated for the methane–water liquid solution [23] using an equation of state. The stability limits suggest that there is a limit to the dissolution of methane in liquid water. However, it is not clear how this limit can be related to the appearance of the hydrate nuclei. In the latter case, there is also a change in the free energy due to the formation of a boundary between the phases in addition to the change in free energy due to the appearance of a certain amount of the new phase. Probably the Gibbs free energy analysis should also include this interfacial energy term. A further analysis of this problem is needed to formulate a method for calculating the supersaturation limits and relating them to the appearance of the nuclei.

## 4. Kinetics of Formation

As mentioned above, the gas hydrate formation is a crystalization process, which is characterized by two distinct phenomena, namely, nucleation and growth. The kinetics of hydrate nucleation are not well understood. It is, however, known to depend on several factors such as thermal and other histories of water [24], presence of foreign particles, state of container wall surface and agitation of the contents. Our studies [18, 19, 20, 21] on the kinetics of hydrate formation are primarily confined to the study of nuclei growth.

### 4.1. THE DRIVING FORCE

In order to develop a kinetic expression for the growth of a hydrate particle, one should first establish the driving force. The identification of the driving force is based on thermodynamic considerations and on the fact that the gas hydrate formation is a crystallization process. In Figure 3 the partial three phase diagram for the ethane–water system is shown. At a given temperature the pressure where the three phases – namely gas, liquid and solid hydrate – exist together is unique. The solid line represents the locus of these points. Formation experiments correspond to particular points on the phase diagram above the three phase equilibrium line and below the vapor pressure curve. For example an experiment performed at $(P_{exp}, T_{exp})$, is shown. The temperature of a formed particle should lie on the equilibrium curve between the points $(P_{eq}, T_{exp})$ and $(P_{exp}, T_{eq})$. The actual position of the point is determined by the heat and mass transfer phenomena around the particle. Namely, if the heat transfer resistance is significant the point approaches $(P_{exp}, T_{eq})$, whereas it approaches $(P_{eq}, T_{exp})$ when the resistance is negligible.

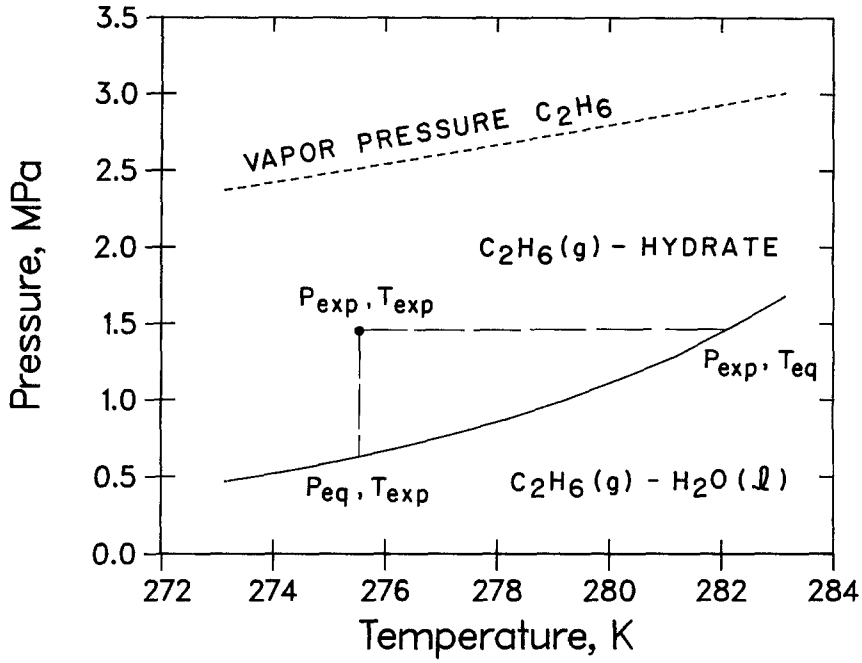


Fig. 3. Identification of the driving force on the partial three phase equilibrium diagram for the ethane gas–liquid water–hydrate system.

Since the three phase equilibrium fugacity represents the minimum fugacity at which hydrates can exist, the driving force for the hydrate crystallization process is given by the difference in the fugacity of the dissolved gas in the liquid and the three phase equilibrium fugacity at the hydrate surface temperature, namely

$$\Delta f = f - f_{eq}. \tag{1}$$

### 4.2. GAS HYDRATE CRYSTAL GROWTH

#### 4.2.1. *Formation from Pure Gases*

The growth of the hydrate particles is envisioned as a two step process, namely,

STEP 1: Diffusion of the dissolved gas from the bulk of the solution to the crystal–liquid interface through the laminar diffusion layer around a particle.

STEP 2: 'Reaction' at the interface, which is an adsorption process describing the incorporation of the gas molecules into the clustered water molecules and the subsequent stabilization of the framework of the structured water.

Since no accumulation is allowed in the diffusion layer around the particle, the rates of the above two processes are equal. Hence, the rate of growth per particle in terms of the overall driving force is obtained,

$$\left(\frac{dn}{dt}\right)_p = K^* A_p (f - f_{eq}) \tag{2}$$

where

$$\frac{1}{K^*} = \frac{1}{k_r} + \frac{1}{k_d}. \tag{3}$$

It is assumed that the outside surface of the surrounding layer is equal to the inside one which is the surface of the particle. It is also assumed that the particles are spherical. The kinetic parameter $K^*$ is an adjustable parameter and it was determined for methane and ethane hydrates by fitting experimental formation data obtained in our laboratory [20].

### 4.2.2. *Formation from Gas Mixtures*

The growth of a hydrate particle from a mixture of methane and ethane is also envisioned to consist of the same two steps. For modelling this two step process for mixtures, we postulate that the rates of diffusion and adsorption of a gas are not affected by the presence of the other gas due to the following reasons:

(a) Both methane and ethane form only structure I gas hydrates.
(b) The gas molecules do not form lattice bonds and it may be assumed that they vibrate and rotate freely within a cavity. The interaction between the water molecules in the lattice and the enclathrated gas molecules is of the van der Waals type and serves to make the structure stable. Hence, there is no qualitative difference in the way the two gases interact with the water in the hydrate phase, although as indicated by the Langmuir constants the interactions are of different magnitude.
(c) In the hydrate phase there are no guest–guest interactions. In the gas phase these interactions have been accounted for by using fugacities rather than pressures.
(d) The incorporation of the gas molecules into the structured water framework depends primarily on their molecular size.

Based on the above, Equation (2) with appropriate definition of the driving force, is used to calculate the rate of consumption of each of the gases for the growth of the hydrate particle. Since the total rate of consumption is equal to the sum of the consumption rates of each component gas, we have for the binary mixture,

$$\left(\frac{dn}{dt}\right)_p = \sum_1^2 \left(\frac{dn_j}{dt}\right)_p = \sum_1^2 K_j^* A_p (f - f_{eq})_j \tag{4}$$

where $K_j^*$ and $(f - f_{eq})_j$ are the individual rate constants and driving forces. The rate constants, $K_j^*$, are those determined from the modelling of the pure component kinetic data. $f_j$ is the fugacity of the component $j$ in the liquid solution and $f_{eq,j}$ is the fugacity of the component $j$ in the gaseous mixture at the three phase equilibrium pressure for the mixture. The gas phase composition is thus comprised indirectly into the above rate expression through the calculation of the fugacities.

### 4.2.3 *Experimental Evaluation of the Model*

For each gas and gas mixture a series of experiments were performed. The experimental equipment is described in detail elsewhere [20, 24, 25]. Under isothermal and isobaric conditions hydrate forming gas is brought in contact with distilled and deionized water in a semi-batch reactor. The liquid phase is in the batch mode. A computer data acquisition and control system enabled on line determination of the number of moles of gas consumed at any point in time.

Once nucleation occurs the hydrate nuclei grow with the forming gas continuously supplied through transport at the gas–liquid interface and subsequent diffusion in the liquid phase. The two film theory, used to describe the mass transfer rate at the gas–liquid interface, was coupled with a homogeneous reaction rate which accounts for the growth of the particles at any point in the reactor. The number and size of the particles in the reactor were estimated with a population balance. The size of the particles is assumed to be sufficiently small compared to the film for gas absorption [20, 21]. The growth of the particles occurs primarily in the film for gas absorption as indicated by Figure 4, where the profile of the fugacity of methane in the liquid phase is shown at the beginning and the end of the experiment as a function of the distance from the gas–liquid interface. The fugacity profile has been calculated using Equation 16 given in [20].

From formation experiments with pure gases the kinetic parameter $K^*$ was estimated by least squares. Subsequently, these parameters were used to predict the formation from gas mixtures. In Figure 5, experimental results of three experiments

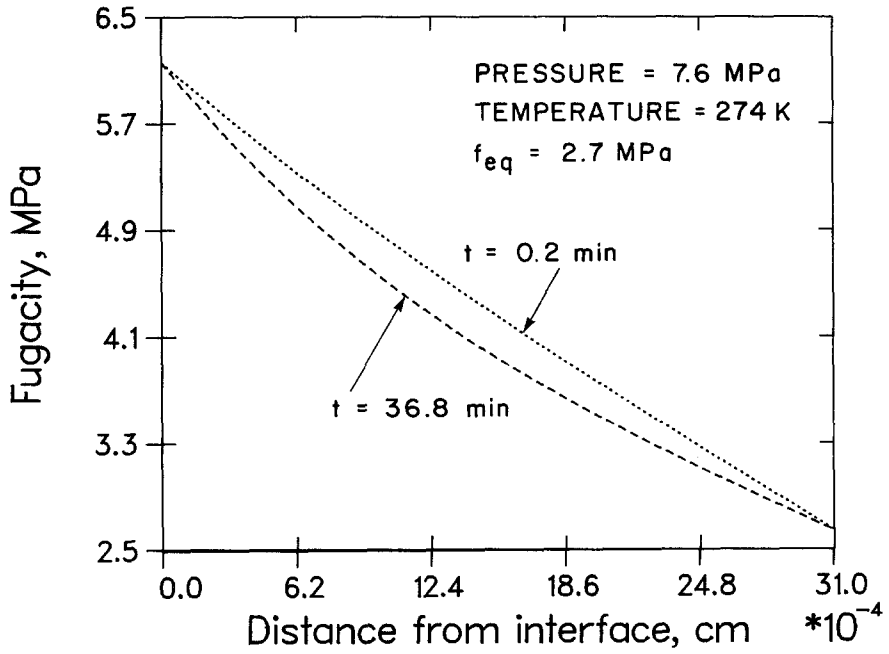


Fig. 4. Methane fugacity profile in the liquid film.

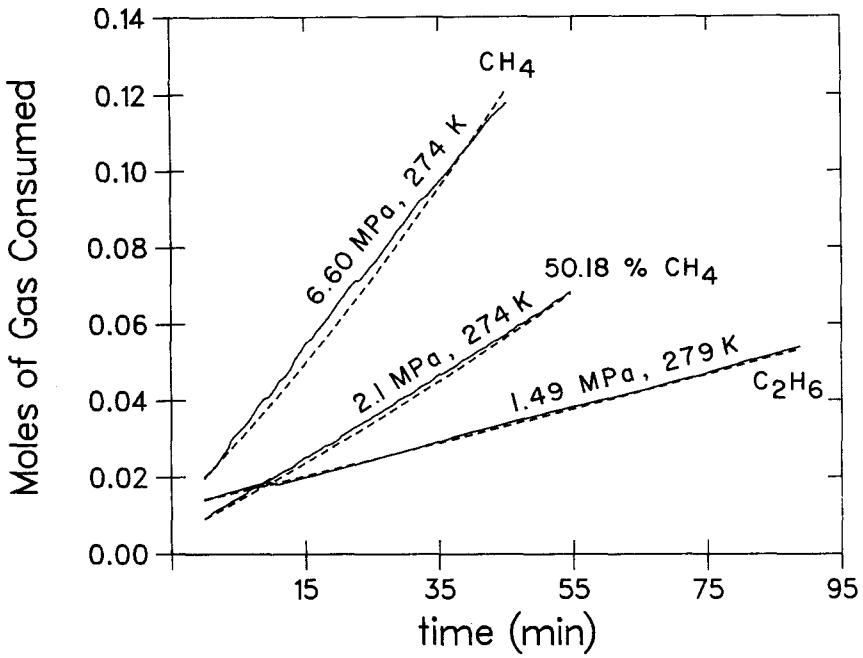


Fig. 5. Experimental and fitted or predicted moles of gas consumed for hydrate formation from methane, ethane and a binary mixture in a semi-batch reactor containing 300 $cm^3$ of distilled water.

are shown as solid lines. The dashed lines represent the fitted curves for methane and ethane, and the model predictions for the binary gas mixture.

The 'reaction' step in hydrate formation is an adsorption process describing the incorporation of the gas molecules into the cluster-like water structure and the subsequent stabilization of the lattice. The kinetic parameter $k_r$, incorporated in the rate constant $K^*$, accounts for the above mechanism of hydrate formation. The parameter $K^*$ is approximately equal to $k_r$ since it is expected that $k_d \gg k_r$ [20]. From the data and the modelling predictions it was realized that the overall gas consumption is strongly proportional to the magnitude of the driving force and not to the pressure itself. In the case of a methane–ethane gas mixture, the three phase equilibrium pressure increases as the methane concentration in the gas mixture increases. As a result, for the same experimental pressure and temperature, the driving force decreases with increasing methane concentration. By comparing two experimental runs at the same temperature the run with higher methane concentration, although at a higher pressure, resulted in smaller consumption rate [21]. The gaseous mixture composition has a strong effect on the rate of hydrate formation as it alters significantly the magnitude of the driving force $(f - f_{eq})_j$ in two ways:

(a) it alters the gas phase fugacity of each component, and
(b) it changes significantly the three phase equilibrium pressure at a given temperature and the magnitude of $f_{eq,j}$.

It should be noted that during the experiments the number of hydrate particles that exist in the reactor were not measured. This number was estimated by a mass balance at the nucleation point. At the present time we cannot find a suitable particle size analyzer to monitor the number of hydrate particles on line primarily due to the high operating pressures. Future research is needed in this area.

## 5. Kinetics of Decomposition

The decomposition of gas hydrates has also been studied. The decomposition process is believed to involve the following two steps:

STEP 1: destruction of the clathrate host lattice at the surface of the particle
STEP 2: desorption of the guest gas molecule from the surface.

These phenomena occur at the surface of the particle and as the decomposition progresses the particle shrinks and the gas generated at the solid surface enters the bulk gas phase. The driving force is given by the difference $f_{eq} - f$, where $f_{eq}$ is the fugacity of the gas at the three equilibrium pressure and $f$ is the fugacity of the gas in the bulk gas phase. Hence, the rate of decomposition for a hydrate particle is given by

$$-\left(\frac{dn_H}{dt}\right)_p = K_d A_p (f_{eq} - f). \tag{5}$$

The hydrate decomposition is an endothermic process and the decomposition constant $K_d$ has an Arrhenius-type temperature dependence. The kinetic parameter was estimated by fitting the experimental data [26]. In Figure 6 the experimental and fitted curves for methane gas hydrate decomposition are shown for five experiments. Again, it is noted that the number of hydrate particles was estimated, rather than being monitored with a particle size analyzer.

## 6. Applications of Intrinsic Kinetics

In general, when the intrinsic kinetic rate constants are available, one need only to describe the transport phenomena in order to simulate complex processes involving the formation or decomposition of gas hydrates. As an example the decomposition of a hydrate block under thermal stimulation [27] was modelled. In this case, the intrinsic kinetic rates are coupled with the heat transfer rate at the decomposing interface (moving boundary) to predict the overall rate of decomposition of the slab. This methodology can be extended for the simulation of processes for natural gas recovery from hydrate reserves. In this case one needs to consider the flow of the gas from the decomposed hydrate and the heat transfer through the porous media. The intrinsic kinetic rate for hydrate formation can be used to simulate many important processes. For example, in the case of a deep water oil well blow out, a gas plume would not be available to pump the oil rapidly towards the surface. The gas will rise mostly in the form of hydrate particles which will be dispersed over a wide area thus causing severe environmental problems [28, 29, 30]. In addition, partial or complete plugging of oil condensate or gas transport pipelines can be modelled when the particle deposition is described. Finally, the formation kinetics are also useful in evaluating water desalination processes.

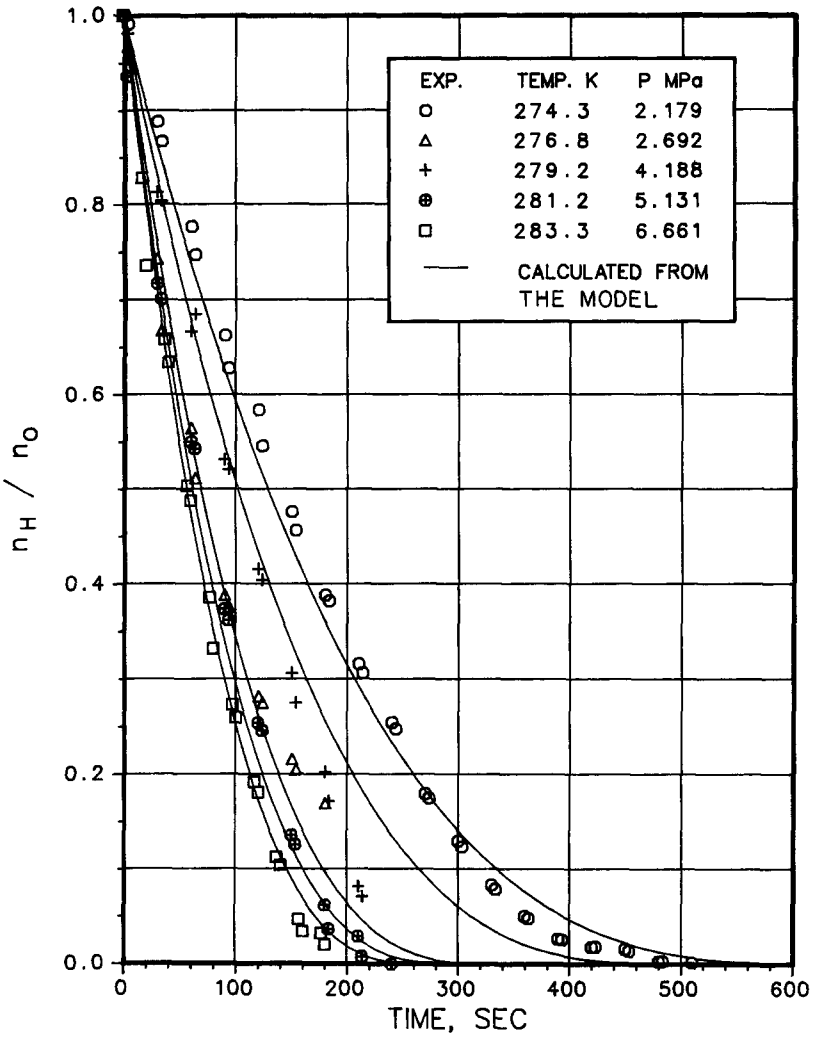


Fig. 6. Normalized moles of methane in the hydrates during decomposition.

## 7. Glossary

$A_p$ surface area of the particles, $m^2$
$f$ fugacity of the gas, MPa
$\Delta f$ driving force, MPa
$k_d$ mass transfer coefficient around the particle, mole/$m^2$ MPa s
$k_r$ 'reaction' rate constant, mole/$m^2$ MPa s
$K^*$ combined rate parameter, mole/$m^2$ MPa s
$K_d$ hydrate decomposition constant, mole/$m^2$ MPa s
$n$ moles of the gas consumed for hydrate formation
$n_H$ moles of methane in the hydrate
$n_0$ moles of methane in the hydrate at time zero

$n_{eq}$ moles of gas dissolved corresponding to three phase equilibrium in 300 $cm^3$ of water
$n^*$ moles of gas dissolved corresponding to vapor–liquid equilibrium in 300 $cm^3$ of water
$P$ Pressure, MPa
$T$ Temperature, K
$t$ time, s

SUBSCRIPTS

$d$ diffusion in Equation 3 and decomposition in Equation 5
eq three phase equilibrium condition
exp experimental
$j$ gaseous component, $CH_4$, $C_2H_6$
$p$ particle
$r$ 'reaction'

## Acknowledgement

Financial support by the National Science and Engineering Research Council of Canada and the Alberta Research Council is greatly appreciated.

## References

1. J. E. D. Davies, W. Kemula, H. M. Powell, and N. O. Smith: *J. Incl. Phenom.* **1**, 3 (1983).
2. Y. F. Makogon: *Hydrates of Natural Gas*, W. J. Cieslewicz Translation PennWell Publishing Co., Tulsa, Oklahoma (1981).
3. E. Berecz and M. Balla-Achs: *Studies in Inorganic Chemistry* 4: *Gas Hydrates*, Elsevier, Amsterdam, 1983 pp. 30–59.
4. D. W. Davidson: *Water – A Comprehensive Treatise*. Vol. 2, ed. F. Franks, Plenum Press, New York. Chap. 3, 1973.
5. D. W. Davidson, S. K. Garg, S. R. Gough, R. E. Hawkins, and J. A. Ripmeester: *Can. J. Chem.* **55**, 3641 (1977).
6. D. W. Davidson, S. R. Gough, J. A. Ripmeester, and H. Nakayama: *Can. J. Chem.* **59**, 2587 (1981).
7. J. H. van der Waals and J. C. Platteeuw: *Adv. Chem. Phys.* **2**, 1 (1959).
8. W. R. Parrish and J. M. Prausnitz: *Ind. Eng. Chem. Proc. Des. Dev.* **11**, 26 (1972).
9. H. J. Ng and D. B. Robinson: *Ind. Eng. Chem. Fundam.* **15**, 293 (1976).
10. V. T. John, K. D. Papadopoulos, and G. D. Holder: *A.I.Ch.E. Journal* **31**, 252 (1985).
11. P. Englezos and P. R. Bishnoi: *A.I.Ch.E. Journal* **34**, 1718 (1988).
12. M. A. Trebble and P. R. Bishnoi: *Fluid Phase Equilibria* **40**, 1 (1988).
13. K. S. Pitzer and G. Mayorga: *J. Phys. Chem.* **77**, 2300 (1973).
14. H. P. Meissner and C. L. Kusik: *A.I.Ch.E. Journal* **18**, 294 (1972).
15. V. S. Patwardhan and A. Kumar: *A.I.Ch.E. Journal* **32**, 1419 (1986).
16. P. Englezos: Ph.D. Thesis, Department of Chemical and Petroleum Engineering, University of Calgary, 1988.
17. P. Englezos, Z. Huang, and P. R. Bishnoi: Presented at the *38th CSChE Conference*. Edmonton, Alberta, October 1988.
18. P. R. Bishnoi, A. A. Jeje, N. Kalogerakis, and R. Saeger: Annual Report to *Energy Mines and Resources*, Ottawa, Canada (1985).
19. P. R. Bishnoi, N. Kalogerakis, A. A. Jeje, P. D. Dholabhai, and P. Englezos: Final Report to *Energy Mines and Resources*, Ottawa, Canada (1986).
20. P. Englezos, N. Kalogerakis, P. D. Dholabhai, and P. R. Bishnoi: *Chem. Eng. Sci.* **42**, 2647 (1987).

21. P. Englezos, N. Kalogerakis, P. D. Dholabhai, and P. R. Bishnoi: *Chem. Eng. Sci.* **42**, 2659 (1987).
22. A. W. Adamson: *Physical Chemistry of Surfaces*, 3rd edition, John Wiley & Sons Inc., N. Y., 1976, pp. 616–618.
23. P. Englezos and P. R. Bishnoi: *Fluid Phase Equilibria* **42**, 129 (1988).
24. A. Vysniauskas and P. R. Bishnoi: *Chem. Eng. Sci.* **38**, 1061 (1983).
25. A. Vysniauskas and P. R. Bishnoi: *Chem. Eng. Sci.* **40**, 299 (1985).
26. H. C. Kim, P. R. Bishnoi, R. A. Heidemann, and S. S. H. Rizvi: *Chem. Eng. Sci.* **42**, 1645 (1987).
27. A. K. M. Jamaluddin., N. Kalogerakis, and P. R. Bishnoi: *The 3rd Chemical Congress of North America*, Toronto, Ont. June 5–10, 1988.
28. B. B. Maini and P. R. Bishnoi: *Chem. Eng. Sci.* **36**, 183 (1981).
29. D. R. Topham: *Chem. Eng. Sci.* **39**, 821 (1984).
30. D. R. Topham: *Chem. Eng. Sci.* **39**, 1613 (1984).